AIP | Applied Physics Letters

Anomalous lattice deformation in GaN/SiC(0001) measured by high-speed in situ synchrotron X-ray diffraction

Takuo Sasaki, Fumitaro Ishikawa, and Masamitu Takahasi

Citation: Applied Physics Letters **108**, 012102 (2016); doi: 10.1063/1.4939450
View online: http://dx.doi.org/10.1063/1.4939450
View Table of Contents: http://scitation.aip.org/content/aip/journal/apl/108/1?ver=pdfcov
Published by the AIP Publishing

Anomalous lattice deformation in GaN/SiC(0001) measured by high-speed *in situ* synchrotron X-ray diffraction

Takuo Sasaki,[1,a)] Fumitaro Ishikawa,[2] and Masamitu Takahasi[1]
[1]*Quantum Beam Science Center, Japan Atomic Energy Agency, 1-1-1 Koto, Sayo, Hyogo 679-5148, Japan*
[2]*Graduate School of Science and Engineering, Ehime University, 3 Bunkyo-cho, Matsuyama 790-8577, Japan*

(Received 27 October 2015; accepted 19 December 2015; published online 4 January 2016)

We report an anomalous lattice deformation of GaN layers grown on SiC(0001) by molecular beam epitaxy. The evolution of the lattice parameters during the growth of the GaN layers was measured by *in situ* synchrotron X-ray diffraction. The lattice parameters in the directions parallel and normal to the surface showed significant deviation from the elastic strains expected for lattice-mismatched films on substrates up to a thickness of 10 nm. The observed lattice deformation was well explained by the incorporation of hydrostatic strains due to point defects. The results indicate that the control of point defects in the initial stage of growth is important for fabricating GaN-based optoelectronic devices. © *2016 AIP Publishing LLC*. [http://dx.doi.org/10.1063/1.4939450]

In all optoelectronic devices composed of GaN-based materials, the initial growth properties of the GaN, i.e., surface morphology, crystal strain, and incorporation of intrinsic point defects, are crucial for their performance.[1–3] In the case of GaN/SiC(0001) heteroepitaxy, these properties should be characterized at the growth temperature because of a large thermal mismatch between the layer and the substrate, which would induce large state variations during cooling.[4] Reflection high-energy electron diffraction (RHEED) is commonly used for *in situ* monitoring in molecular beam epitaxy (MBE), and the surface morphology can be evaluated from changes in the RHEED pattern or intensity.[5,6] Furthermore, this technique can provide the lattice parameter along the in-plane direction, which is estimated from the spacing between streaks.[7,8] However, conventional *in situ* monitoring is insensitive to the lattice parameter along the surface normal direction, knowledge of which is necessary to estimate the initial crystal strain more precisely. Point defects during the initial growth are important since they directly affect the electrical conductivity, carrier recombination, and optical properties.[9–12] Although the point defects (vacancy, antisite, and interstitial defects)[13–16] and their relation to the crystal strain have been extensively studied,[17] previous studies have mainly dealt with GaN films sufficiently thick to be regarded as bulk crystal. Therefore, there has been no report on the initial strain involving the point defects. In this study, *in situ* synchrotron X-ray diffraction (*in situ* XRD) was conducted to measure the lattice parameters of GaN in both the in-plane and out-of-plane directions. The combined use of a high-brilliance synchrotron radiation source and a two-dimensional (2D) detector has enabled high-speed measurements with atomic-scale resolution. Using this method, we found anomalous lattice deformation during the initial growth of GaN, and demonstrated that this is due to incorporation of the point defects.

Experiments were performed at the synchrotron radiation facility SPring-8 (Beamline 11XU), using a plasma-assisted MBE system directly coupled to the X-ray diffractometer.[18,19] In the MBE chamber, following the removal of native oxides from the Si-faced 6H-SiC(0001) substrate by high-temperature heating, GaN was directly grown on the substrates. X-rays with an energy of 20 keV were focused to a size of $0.1 \times 0.1\,\mathrm{mm}^2$ by a four-blade slit. The diffracted X-ray signals were detected by a 2D detector (PILATUS 100 K) with an angular resolution of 0.014°. As shown in Fig. 1(a), while the GaN film was being grown on SiC, 2D reciprocal space maps (RSMs) around the SiC-103 Bragg reflection were measured with the sample rotated about the surface normal η axis by $\pm 1.2°$. A single scan took 7 s, which corresponded to the growth of 0.5-ML thick GaN. The surface morphology was checked by RHEED during and after the growth of GaN. It is known that the initial growth mode of GaN largely depends on growth temperature and III/V flux ratio, and can involve 2D growth, three-dimensional (3D) growth, or transition from 3D to 2D growth, as shown in Fig. 1(b).[20–22] We investigated four samples grown at various temperatures (660 °C, 675 °C, and 690 °C) and III/V flux ratios (1.5 and 0.4). These growth conditions are marked in Fig. 1(b). In the present study, the III/V flux ratio was calibrated by a series of growth experiments with Ga flux varied and N flux fixed. At a relatively low III/V ratio, the growth rate of GaN increased with the Ga flux. With further increasing Ga flux, however, the GaN growth rate is no longer proportional to the Ga flux and eventually became saturated due to limitation of the N supply. From this transition point, which corresponded to the boundary between the group-III limited and group-V limited growth, the N flux was determined to be 0.2 Å/s. Figure 1(c) shows the evolution of RHEED intensity at a specular position during the deposition and desorption of Ga in UHV. The deposition time of Ga was 30 s. At a deposition rate corresponding to a III/V ratio of 1.5, the RHEED intensity decreased in two steps as soon as the Ga shutter was opened. After the supply of Ga was stopped, the RHEED intensity recovered in two steps. This behavior is in good agreement with literature,[23] indicating that the Ga-bilayer and droplets were formed during the deposition of Ga and that the excessive Ga was thermally reevaporated after the Ga shutter was

a)Electronic mail: sasaki.takuo@jaea.go.jp

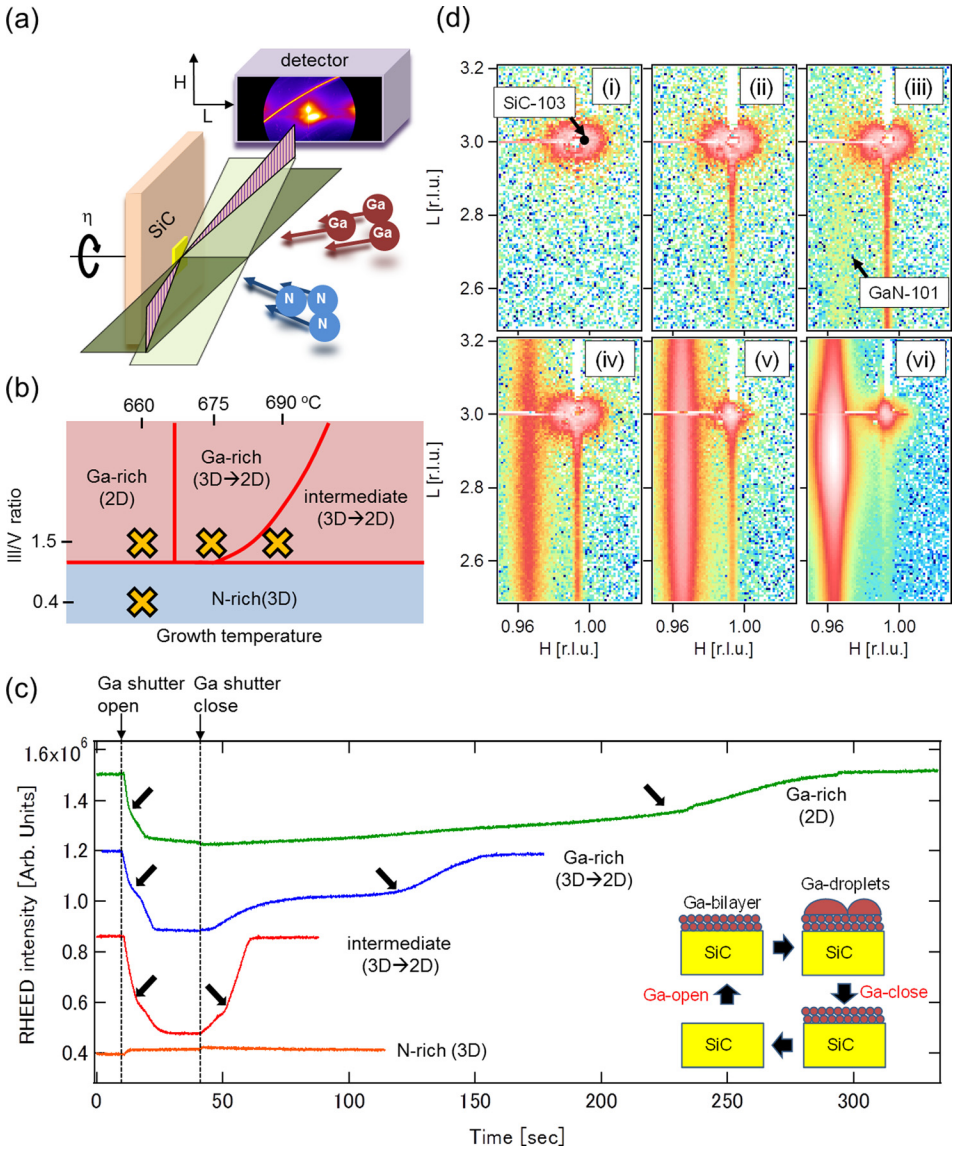

FIG. 1. Schematic of *in situ* XRD during the growth of GaN on the SiC substrate (a), and growth regimes of the GaN as a function of the growth temperature and III/V ratio (b). Growth conditions used in this study are indicated by crosses. Evolution of RHEED intensity during the deposition and desorption of Ga is shown in (c). The N source was not supplied throughout this monitoring. The kinks due to the two-step process are indicated by arrows and corresponding surface structures are schematically shown in the inset. Typical *in situ* RSMs at the growth temperature of 675 °C and Ga-rich conditions are indicated in (d). GaN thicknesses are (i) 0 (before growth), (ii) 0.5, (iii) 0.8, (iv) 1.0, (v) 2.1, and (vi) 10 nm.

closed, as illustrated in the inset. In contrast, the RHEED intensity did not change at a deposition rate corresponding to a III/V ratio of 0.4, suggesting incoming Ga is readily desorbed so that Ga was not accumulated on the surface.

Typical RSMs at GaN thicknesses of 0 to 10 nm at the growth temperature of 675 °C and Ga-rich conditions are shown in Fig. 1(d). The horizontal and vertical axes indicate reciprocal lattice coordinates in the in-plane (H) and surface normal (L) directions, respectively, corresponding to the lattice constants of SiC at the growth temperature.

Figure 2 shows the evolution of the position of the GaN-101 peak as a function of the film thickness when the GaN was grown under Ga-rich and intermediate conditions. At thicknesses less than 1.0 nm, the diffraction intensity was so weak that the peak position could not be determined. Insets are scanning electron microscopy (SEM) and RHEED images measured after the growth of 90-nm thick GaN. Gallium droplets were not observed in the SEM images although the growth was performed under Ga-rich conditions. We assume that the residual Ga droplets on the surface were evaporated while the samples were annealed at the growth temperature for several minutes for post-growth XRD measurements.

At a growth temperature of 660 °C (Fig. 2(a)), the RHEED pattern was almost streaky throughout the growth, which was identified as 2D layer growth. However, as shown in the inset, many surface pits were observed by SEM after the growth of 90-nm thick GaN. At a temperature of 675 °C, the peak shift in the H direction was much smaller than that at 660 °C, as shown in Fig. 2(b). This sample showed a spotty RHEED pattern from the beginning of the growth, indicating the formation of 3D islands. The spots began to change into streaks at 2 nm and this transition was complete at 5 nm. As shown in the inset, clear streak patterns and a relatively smooth surface were observed after the growth. At a substrate temperature of 690 °C (Fig. 2(c)), the peak position in the L direction was found to increase rapidly than that at 675 °C. Although the RHEED pattern showed a gradual transition from 3D to 2D growth, similar to the growth at 675 °C, spotty features persisted even after growth over the thickness of 10 nm. The surface morphology was characterized by plateaus and valleys, which are typical in high-temperature growth of GaN.[21] Figure 3 shows the results under the N-rich conditions, which are often used in nanowire growth.[24–26] The peak position along the L direction

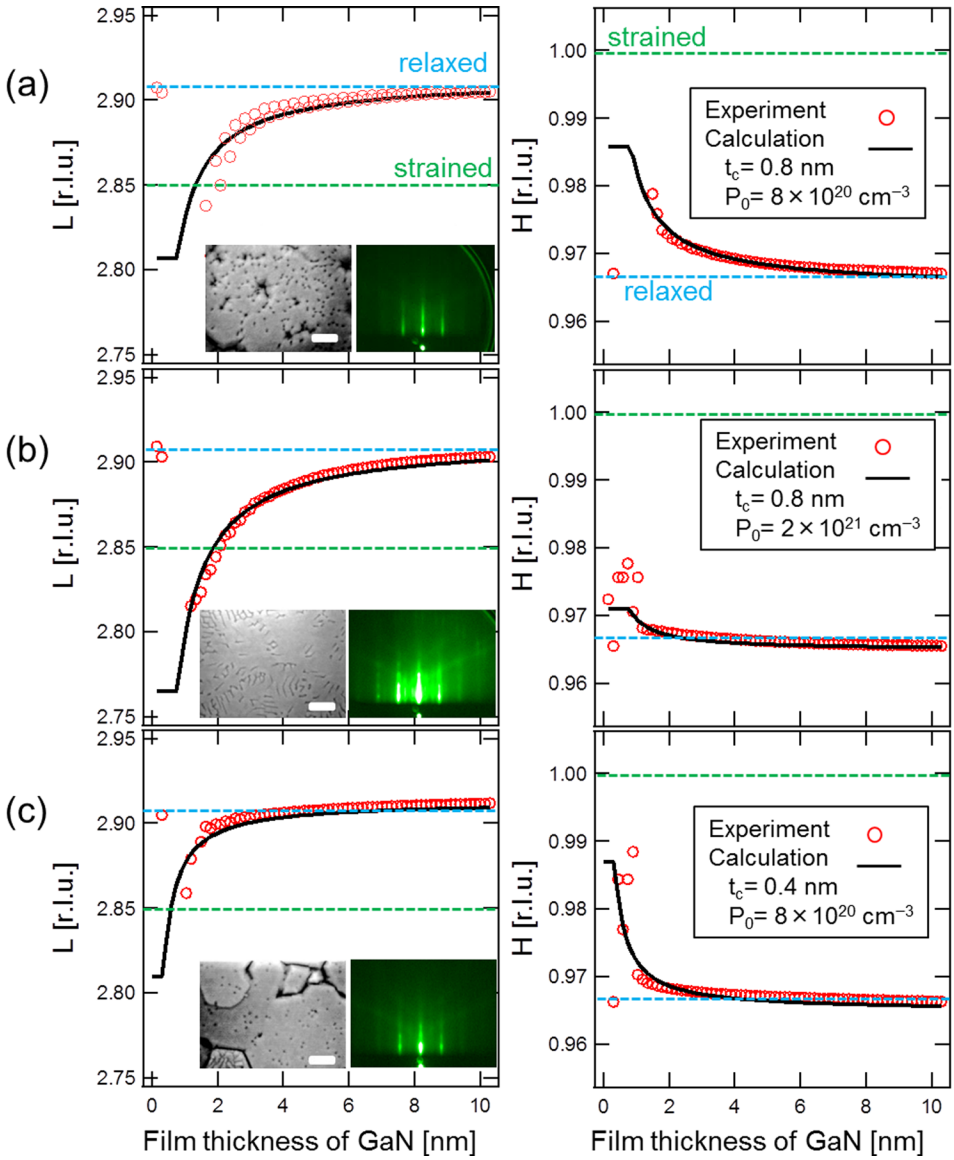

FIG. 2. Evolution of X-ray peak positions in the L and H directions as a function of the film thickness of GaN grown on the SiC substrate under Ga-rich and intermediate conditions. The substrate temperatures were (a) 660 °C, (b) 675 °C, and (c) 690 °C. Insets are SEM images and RHEED patterns along the [11-20] direction after growth of 90 nm thick GaN. In the SEM images, the scale bars correspond to 100 nm. The fully relaxed and fully strained positions were calculated by classical elastic theory and are indicated by dashed lines. Solid lines are calculation results using Equations (1)–(3).

decreased with the GaN thickness. This tendency is contrary to that under the Ga-rich conditions. The RHEED pattern was spotty throughout the growth, which is consistent with the considerably rough surface morphology shown in the inset.

Peak positions calculated by classical elastic theory for fully relaxed and fully strained GaN are shown by the dashed lines in Figs. 2 and 3. In Fig. 2, the change of the peak position is clearly smaller in the H direction than in the L direction. Moreover, in Fig. 3, the peak position in the L direction deviates from the range of the two dashed lines. Their correlation cannot be accounted for by elastic deformation. In previous *ex situ* studies on the strain in thick GaN films, the existence of a hydrostatic strain resulting from point defects

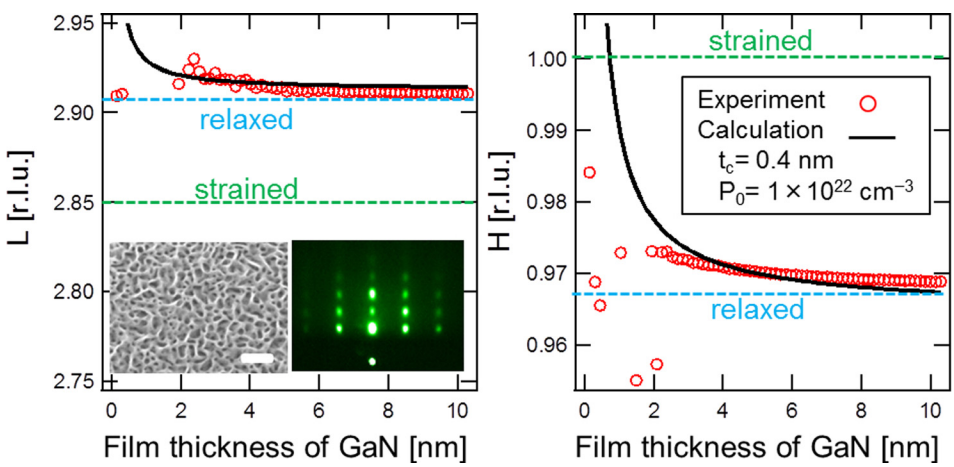

FIG. 3. Evolution of X-ray peak positions in the L and H directions as a function of the film thickness of GaN grown on the SiC substrate under N-rich conditions. Insets are the SEM image and the RHEED pattern along the [11-20] direction after growth of 90-nm thick GaN. In the SEM image, the scale bar corresponds to 100 nm. The fully relaxed and fully strained positions were calculated by classical elastic theory and are indicated by dashed lines. Solid lines are calculation results using Equations (1)–(3).

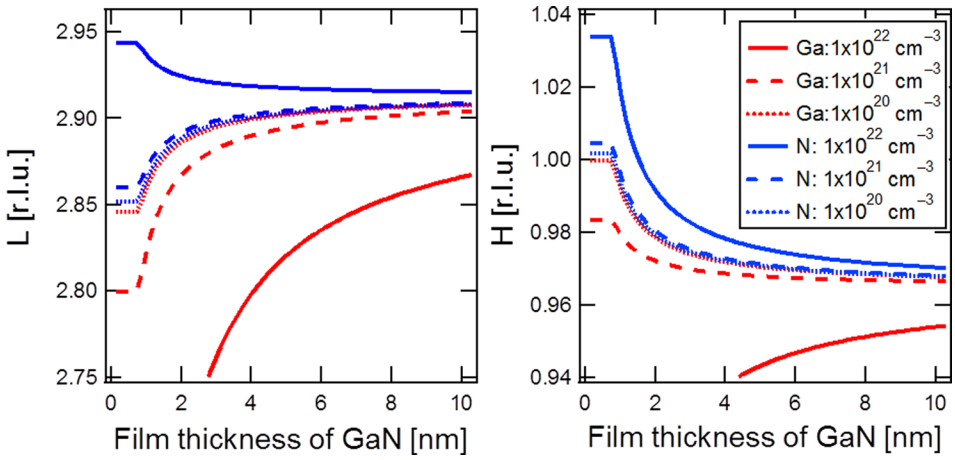

FIG. 4. Calculation results for L and H as a function of the film thickness of GaN grown on the SiC substrate. The initial density of Ga(N) antisites, P_0, was varied in the range of 10^{20} to $10^{22}\,\mathrm{cm}^{-3}$. The critical thickness, t_c, was fixed to be 0.8 nm.

has been reported in addition to the conventional biaxial strain.[17,27–29] Because of the large difference in atomic radii between Ga and N, a high density of point defects is known to be generated in GaN.[30] Kisielowski *et al.*[17] have proposed a strain model, considering both elastic and hydrostatic strains along the surface normal (ε_c) and in-plane (ε_a) directions as follows:

$$\varepsilon_c = (1 - bP)\left(1 + \frac{2\nu}{E}\sigma_a\right) - 1\,,$$
$$\varepsilon_a = (1 - bP)\left(1 - \frac{1-\nu}{E}\sigma_a\right) - 1, \qquad (1)$$

where P is the point defect density, ν is Poisson's ratio, and E is Young's modulus. The coefficient b, which depends on the types of point defects, is expressed as $b = 1/3[1 - (r_s/r_h)^3]A^{-1}$, where r_s and r_h are the atomic radii for the solute and host atoms, respectively, and A is an atomic density, which is $8.8 \times 10^{22}\,\mathrm{cm}^{-3}$ for GaN. The biaxial stress, σ_a, imposed on the grown GaN film by lattice mismatch, can be related to the in-plane lattice parameter, a^{GaN}. Based on van der Merwe's equilibrium model,[31] Kim *et al.*[32] have experimentally determined the thickness dependence of a^{GaN} as $a^{GaN}(t) = a_0^{GaN} + t_c/t(a_0^{SiC} - a_0^{GaN})$, where $a_0{}^{GaN}$ and $a_0{}^{SiC}$ are in-plane lattice constants of unstrained GaN and SiC, respectively, and t_c is the critical thickness. Therefore, the thickness-dependent biaxial stress σ_a can be calculated as follows:

$$\sigma_a = \sigma_0 \frac{a_0^{GaN} - a^{GaN}}{a_0^{GaN} - a_0^{SiC}}, \qquad (2a)$$

where the initial value of the biaxial stress, σ_0, is a misfit stress between GaN and SiC at the growth temperature. Considering that GaN is prone to incorporating point defects in the presence of the biaxial stress, it can be assumed that the point defect density, P, is related to a^{GaN} as follows:

$$P = P_0 \frac{a_0^{GaN} - a^{GaN}}{a_0^{GaN} - a_0^{SiC}}, \qquad (2b)$$

with the initial value of point defect density, P_0. Using Equations (1) and (2), the peak positions in the L and H directions can be derived as follows:

$$L = \frac{3 \times c_0^{SiC}}{\varepsilon_c c_0^{GaN} + c_0^{GaN}}, \qquad H = \frac{a_0^{SiC}}{\varepsilon_a a_0^{GaN} + a_0^{GaN}}, \qquad (3)$$

where $c_0{}^{GaN}$ and $c_0{}^{SiC}$ are lattice constants along the surface normal direction in unstrained GaN and SiC, respectively. Figure 4 shows the results of calculations with varying P_0 for Ga antisites ($r_s = r_{Ga}$, $r_h = r_N$) or N antisites ($r_s = r_N$, $r_h = r_{Ga}$). Though the generation of other intrinsic point defects, such as vacancies or interstitials, is also theoretically predicted in a GaN crystal, Ga(N) antisites are expected to be dominant under Ga(N)-rich growth conditions. The calculation results demonstrate that the hydrostatic strain comes into play for a Ga antisite density higher than $10^{21}\,\mathrm{cm}^{-3}$ and for N antisite density higher than $10^{22}\,\mathrm{cm}^{-3}$. It should be noted that the direction of the peak shift along L reverses with increasing density of N antisites up to $10^{22}\,\mathrm{cm}^{-3}$.

As shown by the solid lines in Figs. 2 and 3, the model based on the incorporation of Ga- or N- antisites provided good fitting results. The critical thickness, t_c, was estimated to be approximately 1 nm, which is in agreement with the theoretical prediction based on Matthews and Blakeslee's model[33] and previous experimental results by RHEED and atomic force microscopy (AFM).[34,35] In contrast, the critical thickness for Stranski–Krastanov (SK) growth of GaN/AlN has been reported to be a similar value, 2 ML (0.5 nm).[36,37] The slight variance in estimated t_c, depending on the growth temperatures, may be due to the initial morphology of GaN. Under Ga-rich conditions, the initial antisite density, P_0, was estimated to be approximately $1 \times 10^{21}\,\mathrm{cm}^{-3}$, which decreased by one order of magnitude over the thickness of 10 nm. By this thickness, hydrostatic strains originating from antisite defects had almost been relieved along with the biaxial strains due to lattice mismatch with the substrate. For undoped growth, it is highly likely that the point defects that induce expansive strains in the initial stage of the growth are gallium antisites. The possibility of other impurities, such as oxygen and carbon, can be eliminated because their atomic radii are smaller than that of gallium. Under N-rich conditions, P_0 was estimated at approximately $1 \times 10^{22}\,\mathrm{cm}^{-3}$, which is higher than that under the Ga-rich conditions. There are several reasons for such a high density of nitrogen antisite defects. First, the Ga/N flux ratio was more distant from stoichiometry in the N-rich conditions than in the Ga-rich

conditions. We have found that increasing the III/V ratio under N-rich conditions (III/V < 1) effectively reduces the initial antisite density.[38] This suggests that careful control of the III/V ratio is important, particularly in the initial stage of growth. Second, a rough surface with a high density of 3D islands facilitates the incorporation of nitrogen because of its large surface area. Third, N antisites in a GaN crystal are energetically more favored than Ga antisites.[39] Finally, volume contraction due to vacancies and impurities other than nitrogen cannot be eliminated.[40] With such unexpected point defects, the concentration of N antisites may be overestimated.

In conclusion, we have performed *in situ* synchrotron XRD measurements to investigate the lattice deformation of GaN films of up to 10 nm grown on SiC(0001). The in-plane and out-of-plane lattice parameters of GaN were found to behave differently from those of the elastically strained film. The point defect model accounted well for the experimental results, indicating that the Ga or N antisite defects, depending on the Ga/N flux ratio, were prone to be formed in the initial stage of GaN growth. The present results show the importance of careful control of stoichiometry in heteroepitaxy of GaN.

This work was performed at BL11XU of SPring-8, Japan, under proposals 2014B3503 and 2015A3503.

[1]S. Nakamura, Jpn. J. Appl. Phys., Part 2 **30**, L1705 (1991).
[2]J. Neugebauer and C. G. Van de Walle, Appl. Phys. Lett. **69**, 503 (1996).
[3]B. K. Ridley, B. E. Foutz, and L. F. Eastman, Phys. Rev. B **61**, 16862 (2000).
[4]D. G. Zhao, S. J. Xu, M. H. Xie, S. Y. Tong, and H. Yang, Appl. Phys. Lett. **83**, 677 (2003).
[5]N. Grandjean and J. Massies, Appl. Phys. Lett. **71**, 1816 (1997).
[6]P. Waltereit, O. Brandt, A. Trampert, M. Ramsteiner, M. Reiche, M. Qi, and K. H. Ploog, Appl. Phys. Lett. **74**, 3660 (1999).
[7]G. Koblmüller, R. Averbeck, H. Riechert, Y.-J. Hyun, and P. Pongratz, Appl. Phys. Lett. **93**, 243105 (2008).
[8]E. Bellet-Amalric, C. Adelmann, E. Sarigiannidou, J. L. Rouvière, G. Feuillet, E. Monroy, and B. Daudin, J. Appl. Phys. **95**, 1127 (2004).
[9]T. Roy, Y. S. Puzyrev, B. R. Tuttle, D. M. Fleetwood, R. D. Schrimpf, D. F. Brown, U. K. Mishra, and S. T. Pantelides, Appl. Phys. Lett. **96**, 133503 (2010).
[10]T. Roy, E. X. Zhang, Y. S. Puzyrev, X. Shen, D. M. Fleetwood, R. D. Schrimpf, G. Koblmueller, R. Chu, C. Poblenz, N. Fichtenbaum, C. S. Suh, U. K. Mishra, J. S. Speck, and S. T. Pantelides, Appl. Phys. Lett. **99**, 203501 (2011).
[11]M. A. Reshchikov, D. O. Demchenko, J. D. McNamara, S. Fernádez-Garrido, and R. Calarco, Phys. Rev. B **90**, 035207 (2014).
[12]M. A. Reshchikov, A. Usikov, H. Helava, and Y. Makarov, Appl. Phys. Lett. **104**, 032103 (2014).
[13]P. Bouguslawski, E. L. Briggs, and J. Bernholc, Phys. Rev. B **51**, 17255 (1995).
[14]I. Gorczyca, A. Svane, and N. E. Christensen, Phys. Rev. B **60**, 8147 (1999).
[15]I. Gorczyca, N. E. Christensen, and A. Svane, Phys. Rev. B **66**, 075210 (2002).
[16]M. A. Reshcikov and H. Morkoç, J. Appl. Phys. **97**, 061301 (2005).
[17]C. Kisielowski, J. Krüger, S. Ruvimov, T. Suski, J. W. Ager III, E. Jones, Z. Liliental-Weber, M. Rubin, E. R. Weber, M. D. Bremser, and R. F. Davis, Phys. Rev. B **54**, 17745 (1996).
[18]M. Takahasi, Y. Yoneda, H. Inoue, N. Yamamoto, and J. Mizuki, Jpn. J. Appl. Phys., Part 1 **41**, 6247 (2002).
[19]T. Sasaki, H. Suzuki, A. Sai, J.-H. Lee, M. Takahasi, S. Fujikawa, K. Arafune, I. Kamiya, Y. Ohsihita, and M. Yamaguchi, Appl. Phys. Express **2**, 085501 (2009).
[20]V. Ramachandran, A. R. Smith, R. M. Feenstra, and D. W. Greve, J. Vac. Sci. Technol. A **17**, 1289 (1999).
[21]B. Heying, R. Averbeck, L. F. Chen, E. Haus, H. Riechert, and J. S. Speck, J. Appl. Phys. **88**, 1855 (2000).
[22]C. D. Lee, A. Sagar, R. M. Feenstra, C. K. Inoki, T. S. Kuan, W. L. Sarney, and L. Salamanca-Riba, Appl. Phys. Lett. **79**, 3428 (2001).
[23]O. Brandt, Y. J. Sun, L. Däweritz, and K. H. Ploog, Phys. Rev. B **69**, 165326 (2004).
[24]E. Calleja, M. A. Sánchez-García, F. J. Sánchez, F. Calle, F. B. Naranjo, E. Muñoz, U. Jahn, and K. Ploog, Phys. Rev. B **62**, 16826 (2000).
[25]J. Ristic, E. Calleja, A. Trampert, S. Fernádez-Garrido, C. Rivera, U. Jahn, and K. H. Ploog, Phys. Rev. Lett. **94**, 146102 (2005).
[26]V. Consonni, M. Knelangen, L. Geelhaar, A. Trampert, and H. Riechert, Phys. Rev. B **81**, 085310 (2010).
[27]H. Harima, J. Phys.: Condens. Matter **14**, R967 (2002).
[28]U. T. Schwauz, P. J. Schuck, M. D. Mason, R. D. Grober, A. M. Roskowski, S. Einfeldt, and R. F. Davis, Phys. Rev. B **67**, 045321 (2003).
[29]A. Krost, A. Dadgar, J. Bläsing, A. Diez, T. Hempel, S. Petzold, J. Christen, and R. Clos, Appl. Phys. Lett. **85**, 3441 (2004).
[30]J. Neugebauer and C. G. Van de Walle, Phys. Rev. B **50**, 8067 (1994).
[31]J. H. van der Merwe, Surf. Sci. **31**, 198 (1972).
[32]C. Kim, I. K. Robinson, J. Myoung, K. Shim, M.-C. Yoo, and K. Kim, Appl. Phys. Lett. **69**, 2358 (1996).
[33]J. W. Matthews and A. E. Blakeslee, J. Cryst. Growth **27**, 118 (1974).
[34]K. H. Ploog, O. Brandt, H. Yang, B. Yang, and A. Trampert, J. Vac. Sci. Technol. B **16**, 2229 (1998).
[35]K. Jeganathan, M. Shimuzu, H. Okumura, F. Hirose, and S. Nishizawa, Surf. Sci. **527**, L197 (2003).
[36]C. Adelmann, B. Daudin, R. A. Oliver, G. A. D. Briggs, and R. E. Rudd, Phys. Rev. B **70**, 125427 (2004).
[37]J. Brown, F. Wu, P. M. Petroff, and J. S. Speck, Appl. Phys. Lett. **84**, 690 (2004).
[38]T. Sasaki, F. Ishikawa, and M. Takahasi "Dependence of lattice deformation on III/V flux ratio in GaN/SiC grown by MBE" (unpublished).
[39]T. Mattila, A. P. Seitsonen, and R. M. Nieminen, Phys. Rev. B **54**, 1474 (1996).
[40]O. Lagerstedt and B. Monemar, Phys. Rev. B **19**, 3064 (1979).